Spectral Properties of Fog Over the Malaspina Glacier, Alaska, in Comparison to Snow, Ice, and Clouds

James P. Ormsby and *Dorothy D. Hall*
Hydrological Sciences Branch, Laboratory for Terrestrial Physics, Goddard Space Flight Center, Greenbelt, MD 20771

ABSTRACT: Analysis of Landsat 5 Thematic Mapper (TM) data of the Malaspina Glacier in southeastern Alaska has shown that fog overlying the glacier ice has reflectance characteristics similar to the ice below and that the spectral reflectance of fog can be different from other types of clouds. Fog is more reflective in the visible and near-infrared wavelengths compared to snow, ice, and cumulus clouds. The differentiation between clouds, fog, and the ice below can be enhanced by combining TM bands in the visible part of the spectrum.

INTRODUCTION

IT HAS BEEN SHOWN that polar clouds or haze due to their tenuous nature " . . .*often present only minimal contrast over* the ice surface as seen from space (and thus change the planetary radiation budget relatively little), but they do affect the radiation flux divergence in the atmospheric column and must be represented realistically in model simulations of polar climate" (WMO, 1988).

Thus, there is a need to detect and locate accurately areas where such features occur. Location of fog and thin clouds is also important for interpretation for remotely sensed imagery. This is especially true over snow-and ice-covered terrain where clouds can be confused with snow and ice. Fog is prevalent in many snow- and ice-covered areas, resulting in difficulty in interpretation of the features below.

A Landsat 5 Thematic Mapper (TM) scene of southeastern Alaska (7 August 1985, scene I.D. Y5052420004X0) was obtained to study the surficial expression of the Malaspina Glacier. The Malaspina Glacier (60°N, 140° 30′W) is a piedmont-type glacier which is composed of three lobes fed by numerous valley glaciers of the St. Elias Mountains. Inspection of the Landsat digital data of the main lobe of the Malaspina Glacier, the Agassiz lobe, revealed the presence of a feature which obliterated portions of the surface. Upon initial inspection, this feature appeared to have spectral characteristics of both cumulus clouds and snow. Further analysis indicated that the feature was probably fog. (Hereafter it will be referred to as fog.) Analysis of meterological data in conjunction with visible (TM bands 2 and 3, 0.52 to 0.60 μm and 0.63 to 0.69 μm, respectively) and near-infrared (TM band 4, 0.76 to 0.90 μm) digital data revealed that this fog was more reflective than snow, ice, or the cumulus clouds nearby. In the longer wavelength, middle infrared region (TM bands 5 and 7, 1.55 to 1.75 μm and 2.08 to 2.35 μm, respectively) and thermal infrared region (TM band 6, 10.40 to 12.50 μm) this feature was found to have spectral properties similar to ice. Thus, TM bands 2 and 3 may allow fog, snow and ice, and clouds to be distinguished.

BACKGROUND

The Malaspina Glacier covers an area of approximately 2650 km^2 and may reach thicknesses between 500 to 1000 m (Allen and Smith, 1953). The ice in the Agassiz lobe is rather smooth compared to the adjacent interlobate areas which are deeply crevassed. This has been observed using Landsat Multispectral Scanner (MSS), Synthetic Aperture Radar (SAR) satellite data (Hall and Ormsby, 1983), and side-looking airborne radar (Molnia and Jones, 1989). The distinctive moraine pattern in the Agassiz lobe is caused by intense deformation from compressional flow as the ice descends from an elevation of about 1200 m to the coastal area where it spreads out onto a much flatter but gently sloping area (Sugden and John, 1976).

PROBLEM

The surface of the Agassiz lobe of the Malaspina Glacier consists of a unique moraine pattern (Figure 1). This pattern was not clearly visible on the 7 August 1985 TM scene, but is clearly visible on previous Landsat scenes acquired in June, August, and September of 1984 and in August 1987. Because of meteorological conditions, it appears highly unlikely that fresh snow is obscuring the glacier surface. TM band 5 (1.55 to 1.75 μm) which is often considered a snow/cloud discriminator band (Dozier, 1984; 1989) here showed a similar response for the "fog" and ice.

METEOROLOGICAL DATA

Yakutat, Alaska (50°31′ N latitude, 139°40′ W longitude) is the closest meteorological station to the Malaspina Glacier. It is about 55 km from its base, across Yakutat Bay (Figure 2). The meteorological data consist of reports every three hours for Yakutat for August 1985 (NOAA, 1985a), radiosonde/rawinsonde observations for 6-8 August 1985 (NOAA, 1985b) at 0000 GMT and 1200 GMT, and Climatological Data for Alaska (NOAA, 1985c).

The Landsat TM scene was acquired at approximately 2000 GMT. Yakutat reported 2/10 sky cover, unlimited ceiling, 80 km visibility, and an air temperature of 14.4°C at 2000 GMT, the time of the satellite overpass. The winds were from the SSW (210°) at 3.6 m sec^{-1}.

The radiosonde data from Yakutat were obtained at 1200 GMT on 7 August 1985 and 0000 GMT on 8 August 1985, 8 hours before and 4 hours after the satellite overpass, respectively. A temperature inversion was present below approximately 950 mb at the time of both observations.

Prior to the 7 August 1985 Landsat overpass, the last snowfall at Yakutat, Alaska occurred on 14 May 1985 and left 4.1 cm of snow on the ground with all snow disappearing by 16 May 1985. For the month of July the average minimum temperature was 9.1°C with the range being 4.4 to 11.7°C. On one of the two days when the minimum temperature was 4.4°C, 28 July 1985, 0.15 cm of precipitation, in the form of rain, was reported. For August, prior to the satellite overpass, the minimum temperature was 4.4°C with an average of 7.8°C for the first seven days (NOAA, 1985c). If we assume an adiabatic lapse rate of 0.6°C/100 m (Blair and Fite, 1965), the air temperature over the

PHOTOGRAMMETRIC ENGINEERING & REMOTE SENSING,
Vol. 57, No. 2, February 1991, pp. 179–185.

0099-1112/91/5702–179$03.00/0

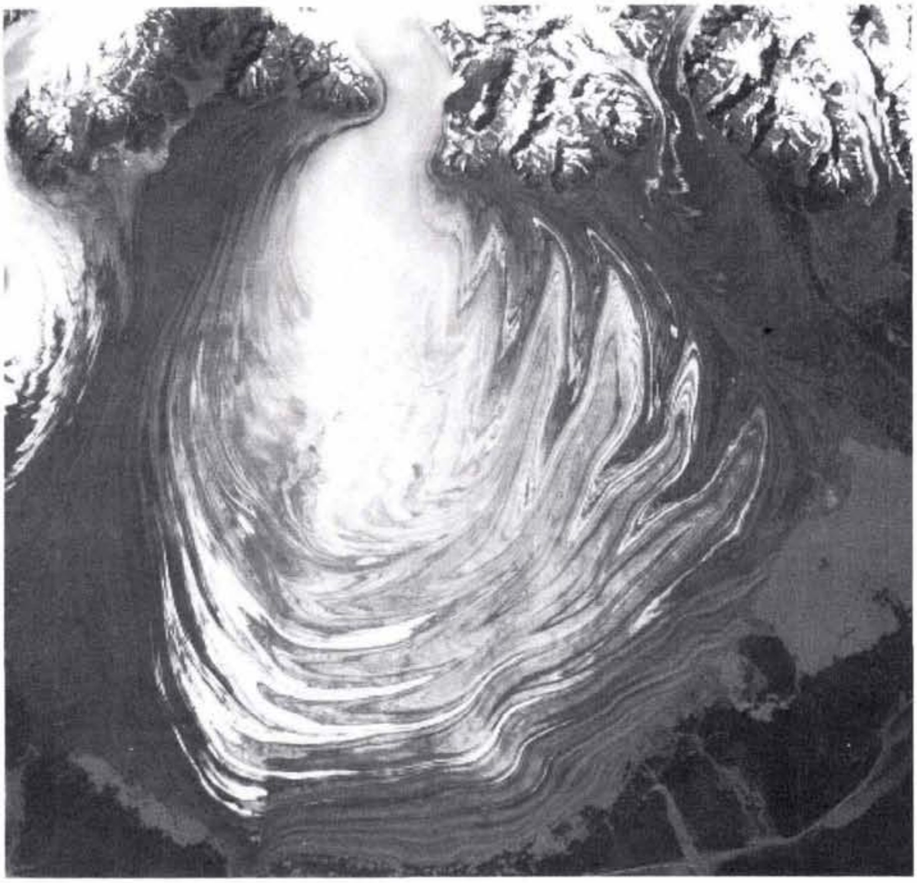

FIG. 1. Landsat MSS image (24 August 1979, scene I.D.# 21675-19482) showing distinctive surface pattern of the Malaspina Glacier.

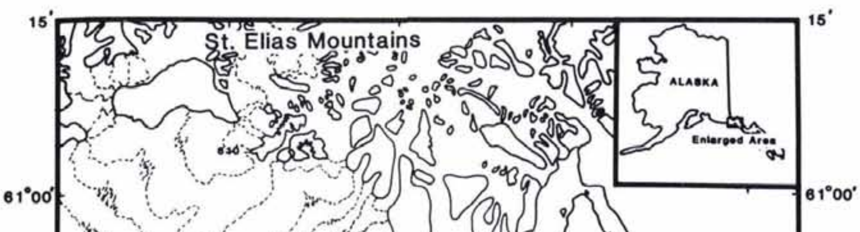

FIG. 2. Map showing the location of the Malaspina glacier and topographic detail of the glacier surface.

glacier would still have been above freezing during the month of July through 7 August 1985. Thus, it is unlikely that a significant amount of fresh snow fell on the glacier during this period.

However, snow can linger on the surface of the Malaspina Glacier for quite a while. In September 1988, snow was observed by B. Molnia (personal communication, 1989) to be present on the Agassiz lobe, but it was restricted to crevasses at lower elevations. Snow was also observed on much of the surfaces near passes. A possible reason snow was observed on the glacier surface late in September 1988 could be due to the fact that temperatures for September 1988 were much lower than those in August 1985. The average minimum temperature in September 1988 at Yakutat was 3.8°C with a range of −2.8°C to 10°C. On seven days the minimum temperature was less than or equal to 0°C. For the month as a whole there was a −1°C departure from normal. No snow, though, was reported at Yakutat in September 1988. The snow may have lingered from snow which fell earlier in the summer. While snow could have fallen on the glacier during the colder mornings when the lapse rate would have resulted in temperatures below 0°C, the amount of snow remaining on the glacier surface in September 1988 is far less than what would have been needed to obscure the glacier surface as seen in the 7 August 1985 TM scene.

ANALYSIS

Petterssen (1969) defines fog as a cloud that envelops the observer (on the ground) and reduces the horizontal visibility to 1 km or less. While this definition is convenient, there is no physical difference between a stratus cloud and a fog. However, in the 7 August 1985 scene a difference in spectral response, expressed as in-band radiance values ($mW \cdot cm^{-2} \cdot ster^{-1}$) (Markham and Barker, 1986), is apparent (Figure 3). The in-band radiance values for the main portion of this thick fog in the visible wavelengths (TM bands 1 to 3) were very high. When expressed in digital numbers (0 to 255), the sensor was saturated in all three bands. Image saturation over the cumulus clouds (over water and land, Figure 3) or ice occurred only in TM band 1. The radiance values in TM bands 2 and 3 were similar for the cumulus clouds and ice. The radiance values for the cumulus clouds (over water and land), compared with ice, were higher in TM band 2 than in TM band 3. The difference between cumulus clouds and ice increases in TM bands 4 and 5. In TM band 7 the difference in spectral response decreased. The radiance values for the fog remained higher than the ice and cumulus clouds through the visible and near-infrered wavelengths and then had a response similar to the ice for TM bands 5 and 7. The similarity in spectral response of the fog and ice may be due to a combination of reflectance from the fog, and ice beneath thin fog contributing to the reflectance detected by the sensor.

Transects of the spectral data for each of the TM bands were taken horizontally and vertically through the fog and surrounding areas using the TM digital data. This area ranges from an elevation of approximately 400 to 600 m (see Figure 2). Figure 4 (TM band 4) shows the location of each of the individual transects. Figures 5 and 6 illustrate the response for vertical transect B-B′ and horizontal transects E-E′, respectively. Analysis of the horizontal and vertical transects through the fog area and over the ice for band 5 showed a slight increase in response in the fog areas versus the ice areas. A larger vertical scale view of just TM band 5 for the vertical (B-B′) and horizontal (E-E′) transects is shown in Figure 7. The in-band radiances (Markham and Barker, 1986) in the fog areas ranged from 0.006 to 0.016 $mW \cdot cm^{-2} \cdot ster^{-1}$ while over the ice surface they ranged from 0.001 to 0.01 $mW \cdot cm^{-2} \cdot ster^{-1}$.

Yakutat reported fog at 0300 GMT which would have coincided with the strong inversion indicated in the radiosonde data for the early morning (1200 GMT) and is shown in Figure 8A. By mid-afternoon (0000 GMT, 8 August 1985), at the time the next radiosonde data were collected, the inversion was still present between 975 and 955 mb as seen in Figure 8B. The height lies between 338 and 511 m.

At 1200 GMT the relative humidity at Yakutat was 86 percent

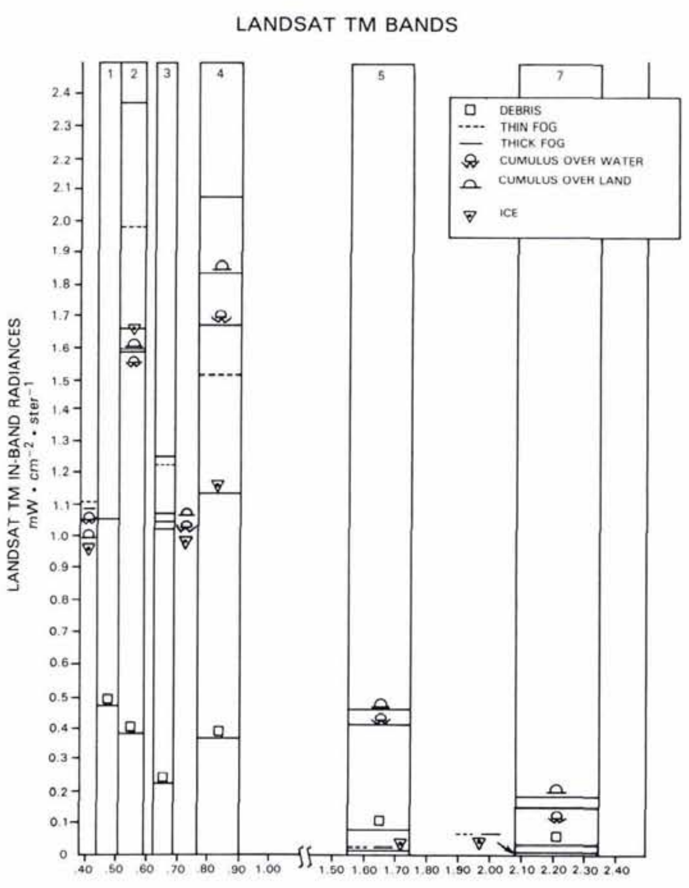

FIG. 3. Plots of in-band radiance (expressed in $mW \cdot cm^{-2} \cdot ster^{-1}$) values for TM bands 1 to 5 and 7 for (▭) debris laden glacier surface, (---), (—) thin and thick fog, (⍜), (⏶) cumulus clouds over water and land, and (▽) ice.

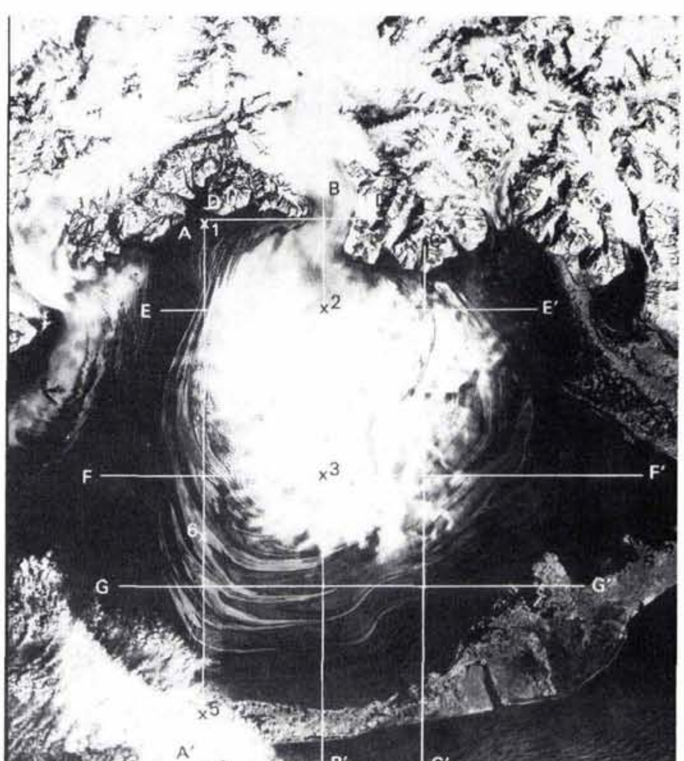

FIG. 4. Map showing the location of the transects used in the study. See Figure 3 for explanation of symbols.

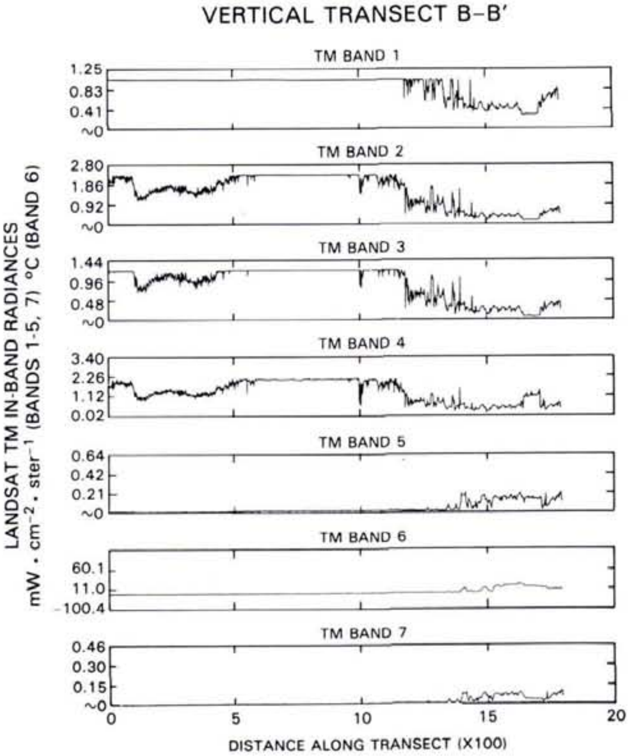

FIG. 5. Vertical transect (B-B') through the fog using all seven TM bands. (Vertical scale: In-band radiances--mW·cm^{-2}·ster^{-1}; horizontal scale: Distance as a function of pixel size--30 metres per pixel).

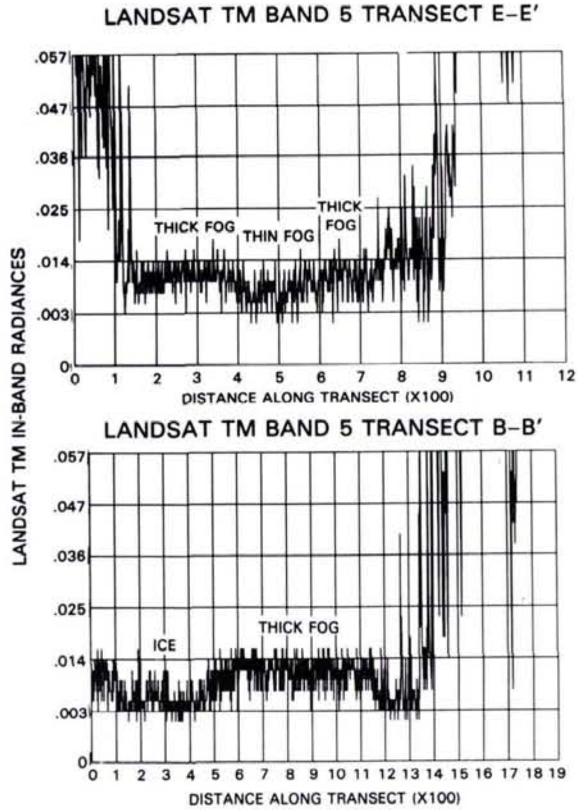

FIG. 7. Enlarged band 5 plots of the vertical (transect B-B') and horizontal (transect E-E') shown in Figure 5 and 6, respectively.

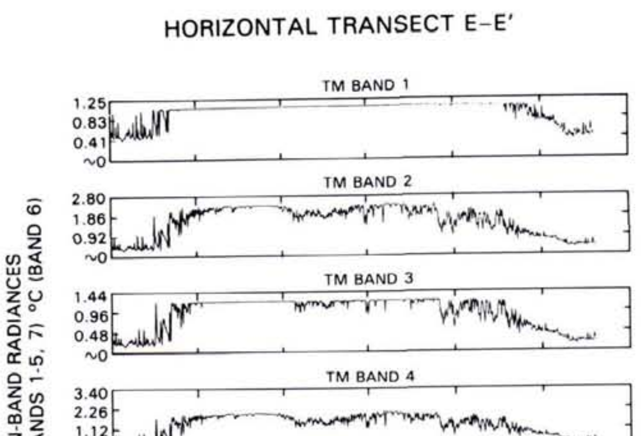

FIG. 6. Same as Figure 5 for horizontal transect (E-E').

at the surface, increasing to 98 percent at 68 m (1007 mb) and decreasing to 91 percent at 126 m (1000 mb) above the surface. By early afternoon, 0000 GMT, the surface temperature rose to 14.4°C, partially eliminating the inversion. Based on the radiosonde data, the humidity remained high at the surface (75 percent) and ranged from 91 percent at 126 m (1000 mb) to 96 percent at 338 m (975 mb). This higher humidity air, if advected over the nearby Malaspina Glacier, would have been cooled sufficiently below the dew point (9.9°C at 1007 mb or 9.7°C at 1000 bm) to produce fog because the ice surface areas are less than or equal to 0°C. Salt particles from the nearby ocean may act as condensation nuclei, allowing condensation to form before the air becomes saturated. Fog can form when the relative humidity is less than 100 percent (Miller, 1966; Petterssen, 1969).

DROPLET AND GRAIN SIZES OF CLOUDS, FOG, ICE, AND SNOW

Snow is highly reflective in the visible wavelengths (Dozier *et al.*, 1981; Dozeir, 1984; 1989; Orheim and Lucchitta, 1987), frequently saturating in TM bands 1, 2, and 3 (0.45 to 0.52 μm, 0.52 to 0.60 μm, and 0.63 to 0.69 μm, respectively). Saturation occurs when the digital numbers (DNs), which range from 0 to 255, are 255. Saturation is less of a problem with the longer wavelength, TM band 4, and is not a problem in the middle-infrared, bands 5 (1.55 to 1.75 μm) and 7 (2.08 to 2.35 μm), in which reflectance over snow and ice is generally very low. This is thought to be due to the larger grain size of ice and snow in relation to the size of cloud droplets (Dozier, 1984; Orheim and Lucchitta, 1987). Water clouds (e.g., cumulus), on the other hand, are brighter than ice clouds (e.g., cirrus) in bands 5 and 7 (Warren, 1982) as seen in Figure 9. As a "snow cloud discrim-

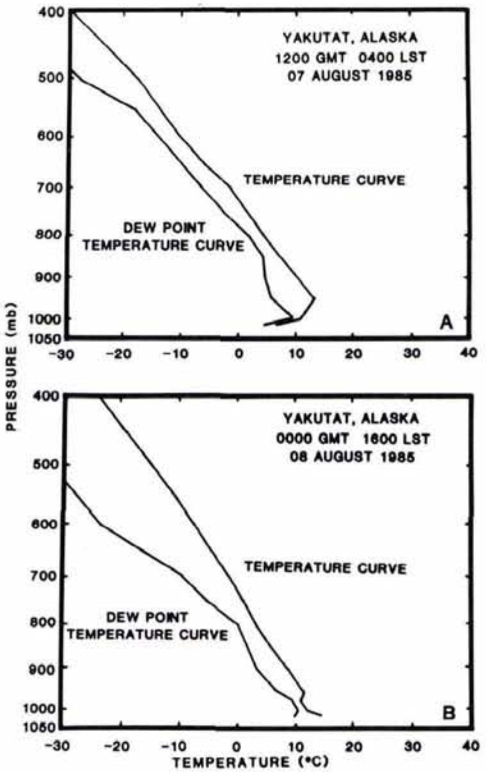

FIG. 8. Temperature versus pressure curves for Yakutat, Alaska, (A) before (1200 GMT, 7 August 1985) and (B) after (0000 GMT, 8 August 1985) the Landsat 5 overpass (2000 GMT, 7 August 1985).

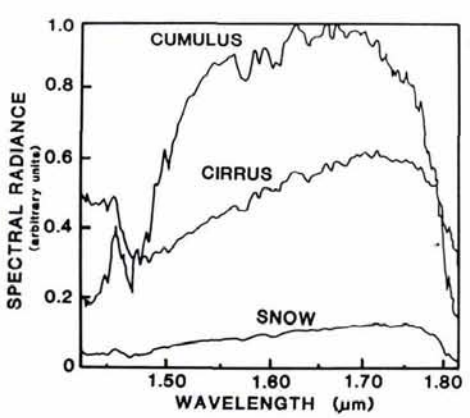

FIG. 9. Relative reflectance of snow and clouds versus wavelength obtained from aircraft observations. Figure redraw from Warren (1982).

inator," the middle-infrared region (1.6 μm) cannot be used to distinguish between thin cloud cover over bare ground and snow cover (Warren, 1982). They are best distinguished in the visible region using a bi-spectral approach. In contrast, Swain and Davis (1978) indicated that, because sunlight is non-selectively scattered by clouds in the reflective region (0.3 to 3.0 μm), there would be a high, uniform spectral response for clouds versus snow in the middle-infrared wavelengths.

Fog, as defined by Pruppacher and Klett (1978), is characterized by relatively low water content (generally less than 0.1 g m^{-3}), drop sizes between 0.5 μm and a few tens of micrometres, and small number concentration (1 cm^{-3} to a few hundred cm^{-3} if drops less than 1 μm are disregarded). Byers (1965) shows graphs of size distribution for advection and radiation fogs obtained near Oslo, Norway, by Pedersen and Todsen (1960). The diameters of the water droplets ranged from 0.001 mm to approximately 0.04 mm and 0.001 mm to approximately 0.03 mm, respectively. The droplet concentrations varied based on the mechanism of formation, with radiation fog having a greater concentration of smaller diameter particles than advection fog.

To maintain an advection fog, a continuous supply of moist air is needed; otherwise, due to the loss of droplets, a fog would clear itself. The loss of droplets and formation of new drops through cooling is typical of all fogs (Petterssen, 1969). The air flow at Yakutat, approximately 70 km from the middle of the glacier, three hours before the satellite overpass was from the NW (320°) shifting to SSW (210°) toward the glacier at 2000 GMT, the time of the Landsat 5 overpass. The winds off the Gulf of Alaska, in conjunction with the orographic lifting of the moist air over the cold glacier surface, would provide the conditions favorable for fog formation. A certain amount of turbulence is needed in the case of advection fog to cool a thicker layer of air as well as to carry the fog particles to greater heights (Cole, 1970). As indicated earlier, winds were from the SSW at 3.6 m sec^{-1}.

Fletcher (1962) indicated "that clouds with large droplet concentrations consist of small droplets, while those with small droplet concentrations contain many large droplets." Measurements on sea fog by Houghton and Radford (1938) reported by Fletcher indicated a median volume diameter of 0.046 mm. Smaller diameters were found for maritime cumulus (0.03 mm) and continental cumulus (0.01 mm) (Battan and Reitan, 1957).

A recent study by Lala *et al.* (1987) provided data on droplet sizes from a site in Albany, New York. Results were similar to those described above. Their instrumentation was able to record droplet sizes from 0.0005 to 0.008 mm and 0.003 to 0.047 mm. In a shallow fog (approximately 50 m) a few droplet sizes larger than 0.04 mm were observed. In a deeper fog (approximately 130 m), droplet sizes were recorded out to the limit of the instrument 0.047 mm). The shape of the spectra indicated the presence of a considerable number of drops larger than the instrument was capable of measuring.

Fresh snow has a grain size of between 0.01 to 5 mm (Meier, 1964). Old snow ranges from 0.5 to 3 mm and glacier ice 1 mm to greater than 200 mm (Meier, 1964; Molnia, 1989, personal communication). The size distribution of droplets in cumulus clouds, as reported by Battan and Reitan (1957) and Byers (1965) over the continental United States, ranged from a radius of less than 0.005 to less than 0.02 mm. Table 1 summarizes the particle sizes for clouds, fog, snow, and ice.

The reflective properties of snow, ice, and clouds depends, in part, on the size of the particles and the wavelength in which they are observed. In the visible region snow reflectance is not dependent on particle (grain) size, while it is in the red and near-infrared. In the middle-infrared, TM bands 5 and 7, ice is highly absorbtive and snow reflectance is low and sensitive to grain size for small sizes. Water, on the other hand, in TM band 5, is less absorbtive than ice, so water clouds are more reflective than ice clouds (Dozier, 1984; 1989). In the middle-infrared the larger the particle size the less reflective. Fog droplets being larger than cumulus cloud droplets (see Table 1) are less reflective in the middle-infrared.

CONCLUSIONS

Meteorological records indicate that no new snow had fallen since 14 May 1985 at Yakutat, Alaska, the closest weather station to the Malaspina Glacier. In addition, the air temperatures at Yakutat for the previous month were greater than 0°C. Due to this it is believed that fog of varying thickness was obscuring the Agassiz lobe of the Malaspina glacier when the 7 August

TABLE 1. DROPLET/GRAIN SIZES FOR CLOUDS, FOG, SNOW, AND ICE

Medium	Droplet/Grain Size micrometres (μm)	millimetres (mm)	Reference
Clouds			
Cumulus			
Maritime	30	0.03	Battan and Reitan, 1957
Continental	10	0.01	Battan and Reitan, 1957
	<5–20	<0.005–<0.02	Byers, 1965
Fog	10–100	0.01–0.1	Blair and Fite, 1965
Advection	1~40	0.001~0.040	Pedersen and Todsen, 1960
Radiation	1~30	0.001~0.030	Pedersen and Todsen, 1960
Shallow	40	0.040	Lala *et al.*, 1987
Deep	>47	>0.047	Lala *et al.*, 1987
Sea Fog	46	0.046	Houghton and Radford, 1938
Snow			
New	10–5000	0.01–5	Meier, 1964
Old	500–3000	0.5–3	Meier, 1964
Glacier Ice	1,000–200,000	1–200	Meier, 1964; Molnia, personal comm.

1985 Landsat TM data were acquired and that new snow was not obscuring the surface. Because the droplet size of fog particles is larger than that of cloud droplets, the spectral response is expected to be different. In the middle-infrared region of the spectrum the smaller cloud droplets are more reflective than the larger fog droplets. As a result, the fog has a spectral response similar to the larger grain sizes of ice and snow. In addition, if the fog is thin, the spectral response of the ice/snow beneath the fog may contribute to the scene reflectance.

Light winds at 3.6 m sec^{-1} from the SSW (210°), along with moist air advected over the cooler ice surface of the Malaspina Glacier, are conditions favorable to the development of fog and these conditions prevailed on 7 August 1985. While it is likely that snow may remain on the Malaspina Glacier's surface for some time after a snowfall, it seems likely that thin surface snow would melt and snow would be restricted to crevasses and other protected areas after a prolonged period of above 0°C air temperatures. Thus, it is highly unlikely that snow was obscuring the glacier's surficial expression on 7 August 1985.

An observed decreased reflectance in the longer (middle-infrared) wavelengths relative to the shorter wavelengths (TM bands 1 to 3) by larger fog droplets indicates a need to check closely what appears to be a "no cloud" situation over ice and snow covered areas. Evidence herein shows that it may be more difficult than has been recognized previously to distinguish clouds (in all forms, but especially fog) from ice and snow using satellite data.

ACKNOWLEDGMENTS

We would like to acknowledge the efforts of Mr. William Kovalick for his expertise in handling and preparing the data for analysis and Drs. Vincent Salomonson, Darrel Williams, and Bruce Molnia for reviewing the manuscript.

REFERENCES

Allen, C. R., and G. I. Smith, 1953. Seismic and Gravity Investigations on the Malaspina Glacier, *Eos Trans. AGU, 34,* p 755.

Battan, L. J., and C. H. Reitan, 1957. Droplet Size Measurements in Convective Clouds, *Artificial Stimulation of Rain,* (H. Weickmann and W. Smith, editors), New York: Pergamon Press, 184 p.

Blair, T. A., and R. C. Fite, 1965. *Weather Elements,* Prentice-Hall, Inc., Englewood Cliffs, New Jersey, 364 p.

Byers, H. R., 1965. *Elements of Cloud Physics,* The University of Chicago Press, Chicago, Illinois.

Cole, F. W., 1970. *Introduction to Meteorology,* John Wiley and Sons, Inc., New York, 388 p.

Dozier, J., 1984. Snow Reflectance From Landsat-4 Thematic Mapper, *IEEE Trans. Geosci. Remote Sens.* GE-22:323–328.

———, 1989. Spectral Signature of Alpine Snow Cover From the Landsat Thematic Mapper, *Remote Sens. Environ.* 28:9–22.

Dozier, J., S. R., Schneider, and D. F., McGinnis, Jr., 1981. Effect of Grain Size and Snowpack Water Equivalence on Visible and Near-Infrared Observations of Snow, *Water Resources Research* 17:1213–1221.

Fletcher, N. H., 1962. *The Physics of Rainclouds,* Cambridge University Press, Cambridge, England.

Hall, D. K., and J. P. Ormsby, 1983. Use of SEASAT Synthetic Aperature and Landsat Multispectral Scanner Data for Alaskan Glaciology Studies, *Journal of Geophysical Research,* Vol. 88, No. C3, pp. 1597–1607.

Houghton, H. G., and W. H. Radford, 1938. On the Measurement of Drop Size and Liquid-Water Content in Fogs and Clouds, *M.I.T. Papers in Phys. Oceanog. Met. 6.* No. 4.

Lala, G. G., D. R. Fitzjarrald, and M. B. Meyer, 1987. *Fog, Rain, and Aerosol Attenuation in the Atmosphere,* Final Report, US Army Research Office Contract No: DAAG-29-84-K-0050. 60 p.

Markham, B. L., and J. L. Barker, 1986. "Landsat MSS and TM Post-Calibration Dynamic Ranges, Exoatmospheric Reflectances and AT-Satellite Temperatures", *EOSAT Landsat Technical Notes No. 1,* 3.

Meier, M. F., 1964. Ice and Glaciers, *Applied Hydrology* (V. T. Chow, ed.), Section 16.

Miller, A., 1966. *Meteorology,* Charles E. Merrill Books, Inc., Columbus, Ohio, 128 p.

Molnia, B. F., and J. E. Jones, 1989. View Through Ice: Are Unusual Airborne Radar Backscatter Features from the Surface of the Malaspina Glacier, Alaska, Expressions of Subglacial Morphology?, *Eos, Transactions, American Geophysical Union, Vol. 70,* No. 28, pp. 701-710.

NOAA, 1985a. *Local Climatological Data Monthly Summary, August, Yakutat, Alaska,* National Climatic Data Center, Asheville, North Carolina.

———, 1985 b. *Radiosonde/Rawinsonde Data, August 7-8, 1985, Yakutat, Alaska,* National Climatic Data Center, Asheville, North Carolina.

———, 1985 c. *Climatological Data Alaska,* National Climatic Data Center, Vol. 71, No. 8, Asheville, North Carolina.

Orheim, O., and B. K. Lucchitta, 1987. Snow and Ice Studies by Thematic Mapper and Multispectral Scanner Landsat Images, *Annals of Glaciology,* Vol. 9, pp. 109–118.

Pedersen, K., and M. Todsen, 1960. *Norske Videnskaps-Akad.,* Geofys. Pub., 21, No. 7.

Petterssen, S., 1969. *Introduction to Meteorology*, McGraw-Hill Book Co., New York, 333 p.

Pruppacher, H. R., and J. D. Klett, 1978. *Microphysics of Clouds and Precipitation*, D. Reidel Publishing Co., Dordrecht, Holland.

Sugden, D. E., and B. S. John, 1976. *Glaciers and Landscapes*, John Wiley, New York, 376 p.

Swain, P. H., and S. M. Davis (eds.), 1978. *Remote Sensing: The Quantitative Approach*, McGraw-Hill, New York.

Warren, S. G., 1982. Optical Properties of Snow, *Reviews of Geophysics and Space Physics*, Vol. 20, No. 1, pp. 67–89.

WMO, 1988. *Report of the Third Session of the Working Group on Sea Ice and Climate*, WMT/TD No. 272, WCRP-18, Oslo, Norway.

(Received 4 December 1989; accepted 12 February 1990; revised 23 May 1990)

Forthcoming Articles

K. F. Adkins and *J. G. Lyon*, Use of Aerial Photographs to Identify Suitable GPS Survey Stations.
Patrick A. Agbu and *Egide Nizeyimana*, Comparisons between Spectral Mapping Units Derived from SPOT Image Texture and Field Soil Map Units.
Eric W. Augenstein, *Douglas A. Stow*, and *Allen S. Hope*, Evaluation of SPOT HRV-XS Data for Kelp Resource Inventories.
Emmanuel P. Baltsavias and *Dirk Stallmann*, Trinocular Vision for Automatic and Robust Three-Dimensional Determination of the Trajectories of Moving Objects.
David G. Barber and *Ellsworth F. LeDrew*, SAR Sea Ice Discrimination Using Texture Statistics: A Multivariate Approach.
Eugenia M. Barnaba, *Warren R. Philipson*, *Arlynn W. Ingram*, and *Jim Pim*, The Use of Aerial Photographs in County Inventories of Waste-Disposal Sites.
D. S. Bhargava and *Dejene W. Mariam*, Effects of Suspended Particle Size and Concentration on Reflectance Measurements.
John M. Briggs and *M. Duane Nellis*, Seasonal Variation of Heterogeneity in the Tallgrass Prairie: A Quantitative Measure Using Remote Sensing.
Doug C. Brockelbank and *Ashley P. Tam*, Stereo Elevation Determination Techniques for SPOT Imagery.
Roger R. Chamard, Snake Oilers and Ethics.
Pat S. Chavez, Jr., *Stuart C. Sides*, and *Jeffrey A. Anderson*, Comparison of Three Different Methods to Merge Multiresolution and Multispectral Data: Landsat TM and SPOT Panchromatic.
Jean Chorowicz, *Jean-Yves Preard*, *Richard Guillande*, *Claude-Roger Morasse*, *Daniel Prudon*, and *Jean-Paul Rudant*, Dip and Strike Measured Systematically on Digitized Three-Dimensional Geological Maps.
P. K. Chua, *A. H. W. Kersley*, *J. K. Ridley*, *W. Cudlip*, and *C. G. Rapley*, The Determination and Use of Orthometric Heights Derived from the Seasat Radar Altimeter over Land.
William M. Ciesla, Ethics in Photogrammetry and Remote Sensing: A Perspective from a Natural Resource Specialist.
Jeffrey D. Colby, Topographic Normalization in Rugged Terrain.
Liping Di and *Donald C. Rundquist*, Instantaneous Three-Channel Image Processing to Facilitate Instruction.
Sanjib K. Ghosh and *Zhengdong Shi*, Evaluating Dynamic Performance of an Analytical Plotter.
Joshua S. Greenfeld, An Operator-Based Matching System.
Nils N. Haag, *Michael H. Brill*, and *Eamon B. Barrett*, Invariant Relationships in Side-Looking Synthetic Aperture Radar Imagery.
Brenton J. Keefer, *James L. Smith*, and *Timothy G. Gregoire*, Modeling and Evaluating the Effects of Stream Mode Digitizing Errors on Map Variables.
T. K. Koo and *Y. B. Aw*, A Three-Dimensional Visualization Approach to Traffic Accident Mapping.
James LaGro, Jr., Assessing Patch Shape in Landscape Mosaics.
Hans Middelkoop and *Lucas L. F. Jansseen*, Knowledge-Based Classification of Satellite Images.
A. J. Naftel and *J. C. Boot*, An Iterative Linear Transformation Algorithm for Solution of the Collinearity Equations.
William R. Niedzwiedz and *Lee W. Ganske*, Assessing Lakeshore Permit Compliance Using Low Altitude Oblique 35-mm Aerial Photography.
Derek R. Peddle and *Steven E. Franklin*, Image Texture Processing and Data Integration for Surface Pattern Discrimination.
Mohammed Yousef H. T. Qari, Application of Landsat TM Data to Geological Studies, Al-Khabt Area, Southern Arabian Shield.
J. Raul Ramirez, Digital Topographic Maps: Production Problems and Their Impact on Quality and Cost.
Eric J. M. Rignot, *Ronald Kwok*, *John C. Curlander*, and *Shirley S. Pang*, Automated Multisensor Registration: Requirements and Techniques.
T. W. Ryan, *P. Sementilli*, *P. Yuen*, and *B. R. Hunt*, Extraction of Shoreline Features by Neural Nets and Image Processing.
S. D. Wall, *T. G. Farr*, *J -P Muller*, *P. Lewis*, and *F. W. Leberl*, Measurement of Surface Microtopography.